cmgh
CELLULAR AND MOLECULAR GASTROENTEROLOGY AND HEPATOLOGY

ORIGINAL RESEARCH

Mesencephalic Astrocyte-derived Neurotrophic Factor Supports Hepatitis B Virus-induced Immunotolerance

Huiyuan Xie,[1,*] Haiyan Deng,[2,*] Xiaoping Yang,[3,*] Xianxian Gao,[2] Shanru Yang,[2] Weiyi Chen,[2] Yixuan Wang,[2] Naibin Yang,[4] Liang Yong,[5] and Xin Hou[2]

[1]Department of Laboratory Medicine, the First Affiliated Hospital of Ningbo University, Ningbo, Zhejiang, P. R. China; [2]Health Science Center, Ningbo University, Ningbo, Zhejiang, P. R. China; [3]Department of Hepatopancreatobiliary Surgery, the First Affiliated Hospital of Ningbo University, Ningbo, Zhejiang, P. R. China; [4]Department of Infection, the First Affiliated Hospital of Ningbo University, Ningbo, Zhejiang, P. R. China; and [5]Laboratory of Stem Cell, the First Affiliated Hospital of Ningbo University, Ningbo, Zhejiang, P. R. China

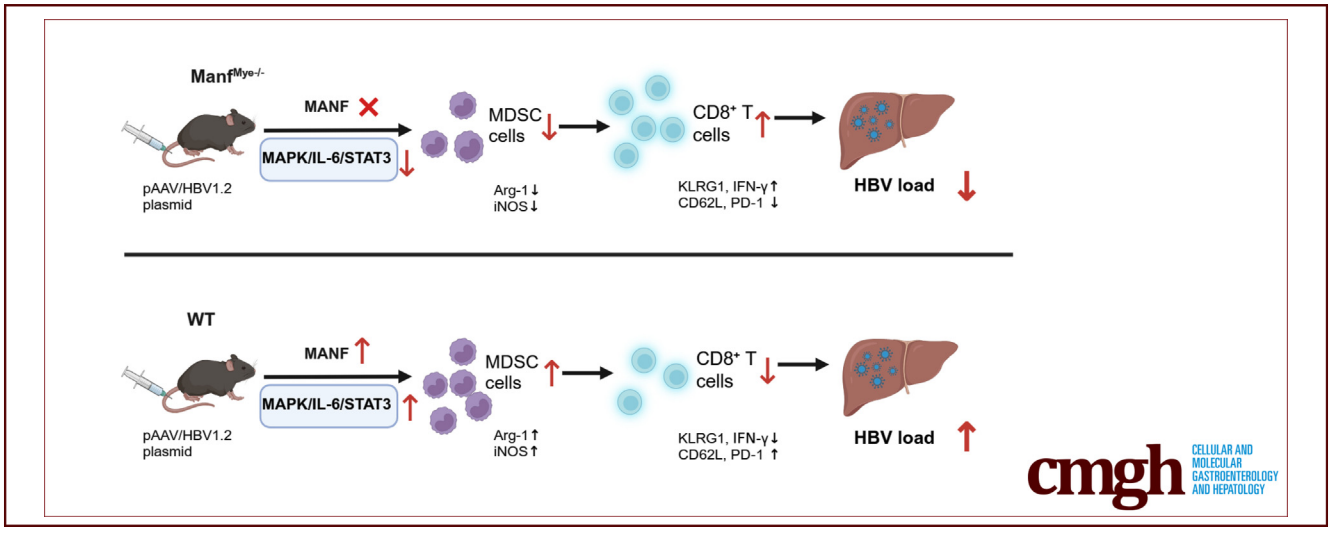

SUMMARY

Our study revealed that mesencephalic astrocyte-derived neurotrophic factor promoted hepatitis B virus-induced immune tolerance by expanding myeloid-derived suppressor cells in the liver through MAPK/IL-6/STAT3 signaling, leading to myeloid-derived suppressor cell-mediated $CD8^+$ T cell exhaustion. Importantly, siRNA targeting mesencephalic astrocyte-derived neurotrophic factor-based vaccination therapy was shown to effectively clear hepatitis B virus.

BACKGROUND & AIMS: The immune tolerance induced by hepatitis B virus (HBV) is a major challenge for achieving effective viral clearance, and the mechanisms involved are not well-understood. One potential factor involved in modulating immune responses is mesencephalic astrocyte-derived neurotrophic factor (MANF), which has been reported to be increased in patients with chronic hepatitis B. In this study, our objective is to examine the role of MANF in regulating immune responses to HBV.

METHODS: We utilized a commonly used HBV-harboring mouse model, where mice were hydrodynamically injected with the pAAV/HBV1.2 plasmid. We assessed the HBV load by measuring the levels of various markers including hepatitis B surface antigen, hepatitis B envelope antigen, hepatitis B core antigen, HBV DNA, and HBV RNA.

RESULTS: Our study revealed that following HBV infection, both myeloid cells and hepatocytes exhibited increased expression of MANF. Moreover, we observed that mice with myeloid-specific MANF knockout ($Manf^{Mye-/-}$) displayed reduced HBV load and improved HBV-specific T cell responses. The decreased HBV-induced tolerance in $Manf^{Mye-/-}$ mice was associated with reduced accumulation of myeloid-derived suppressor cells (MDSCs) in the liver. Restoring MDSC levels in $Manf^{Mye-/-}$ mice through MDSC adoptive transfer reinstated HBV-induced tolerance. Mechanistically, we found that MANF promoted MDSC expansion by activating the IL-6/STAT3 pathway. Importantly, our study demonstrated the effectiveness of a combination therapy involving an hepatitis B surface antigen vaccine and nanoparticle-encapsulated MANF siRNA in effectively clearing HBV in HBV-carrier mice.

CONCLUSION: The current study reveals that MANF plays a previously unrecognized regulatory role in liver tolerance by expanding MDSCs in the liver through IL-6/STAT3 signaling, leading to MDSC-mediated $CD8^+$ T cell exhaustion. *(Cell Mol Gastroenterol Hepatol 2024;18:101360; https://doi.org/10.1016/j.jcmgh.2024.05.008)*

Keywords: HBV; MANF; MDSC.

Hepatitis B virus (HBV) infection is a significant global health problem, with more than 240 million people worldwide chronically infected, primarily in Asia and the South Pacific.[1] This infection can lead to severe liver diseases such as fibrosis, cirrhosis, and hepatocellular carcinoma in 20% to 30% of patients with chronic hepatitis B (CHB).[2] The persistence of chronic HBV infection is due to immune tolerance toward HBV in the liver, which is characterized by defective HBV-specific T cell responses.[3] Several mechanisms have been proposed to explain this functional T cell impairment, including prolonged exposure to high HBV antigen concentrations leading to T cell exhaustion and impaired T cell receptor signaling via the ζ-chain.[4,5] In addition, immunoregulatory cell populations in the liver, including regulatory T cells (Tregs), hepatic dendritic cells, and myeloid-derived suppressor cells (MDSCs), have been reported to play a role in the suppression of HBV-specific $CD8^+$ T cell priming, activation, and proliferation.[5,6]

MDSCs are a heterogeneous cell population derived from myeloid progenitor cells, which can be categorized into two subpopulations, monocytic (M) and polymorphonuclear (PMN) ones. In humans, M-MDSCs are defined as $CD11b^+CD14^+CD15^-$, whereas PMN-MDSC are defined as $CD11b^+CD14^-CD15^+$.[7,8] In mice, M-MDSCs are $CD11b^+Ly6G^-Ly6C^{high}$, and PMN-MDSCs are $CD11b^+Ly6G^{high}Ly6C^{low}$.[7,9] MDSCs are induced and expanded by local cytokines, such as CSF, SCF, IL-6, and VEGF.[10] Recent studies have found a higher percentage of MDSCs in peripheral blood and liver tissue of patients with CHB.[8,11] These MDSCs have been demonstrated to suppress HBV-specific $CD8^+$ T cell response through PD-1–induced IL-10 and indoleamine-2, 3-dioxygenase in patients with CHB,[8,11] as well as by Arg-1 in HBV-carrier mice.[6] Hepatitis B surface antigen (HBsAg) and hepatitis B envelope antigen (HBeAg) were shown to trigger mMDSC expansion[11–13]; however, the underlying mechanism remains to be fully elucidated.

Mesencephalic astrocyte-derived neurotrophic factor (MANF) is an ER luminal protein whose expression and secretion can be induced by ER stress.[14] Emerging studies have demonstrated that MANF plays a role in regulating inflammation.[14,15] Our previous research indicated that MANF facilitates the conversion of pro-inflammatory monocyte-derived macrophages to pro-restorative $Ly6C^{low}$ macrophages, promoting the resolution of liver injury caused by acetaminophen.[16] Notably, recent reports suggest that spliced X-box binding protein-1 and activator protein-1 increase MANF expression in the liver tissues of patients with HBV infection[17,18]; however, the role of MANF in HBV infection has not been fully elucidated. In this study, we investigated the role of MANF in HBV infection using an HBV-harboring mouse model. We found that myeloid cell-derived MANF promotes HBV-induced tolerance by participating in $CD8^+$ T cell exhaustion through IL-6/STAT3–mediated MDSC accumulation. Importantly, siRNA targeting MANF (siMANF)-based vaccination therapy was shown to effectively clear HBV.

Results

Increased MANF Expression in HBV-positive Mouse Model

To investigate the of MANF in HBV persistence, we utilized an HBV-harboring mouse model in which the pAAV/HBV 1.2 plasmid was injected into mice via high pressure in the tail vein to mimic chronic HBV infection.[19,20] Initially, we examined MANF expression in the liver of the HBV-positive mouse. As shown in Figure 1*A*, our findings revealed significantly higher levels of MANF mRNA in the liver tissues of HBV-positive mice compared with the control group. Furthermore, we performed an immunofluorescence analysis to co-stain hepatic myeloid cells and hepatocytes with MANF. As illustrated in Figure 1*B* and *C*, both $CD11b^+$ myeloid cells and $HepPar1^+$ hepatocytes exhibited an increased expression of MANF protein, indicating its involvement in HBV persistence.

MANF Deficiency in Myeloid Cells Promotes HBV Clearance

To investigate the distinct roles of MANF in hepatocytes and myeloid cells, we employed hepatocyte-specific MANF knockout mice ($Manf^{Hep-/-}$) and myeloid-specific MANF knockout mice ($Manf^{Mye-/-}$). These mice were subsequently treated with the pAAV/HBV1.2 plasmid. Compared with wild-type (WT) mice, $Manf^{Mye-/-}$ mice exhibited significantly lower levels of serum hepatitis B surface antigen (HBsAg) and HBeAg at the indicated time points (Figure 2*A* and *B*). Moreover, HBV-positive $Manf^{Mye-/-}$ mice displayed reduced hepatitis B core antigen (HBcAg) protein expression and decreased HBV RNA levels in liver tissues compared with HBV-positive WT mice (Figure 2*C*–*E*). In contrast, $Manf^{Hep-/-}$ mice showed comparable HBV antigens and HBV RNA levels to WT mice. Collectively, these findings suggest that the deficiency of MANF in myeloid cells enhances the immune response against HBV in mice.

MANF Deficiency in Myeloid Cells Alleviates HBV-induced Immunotolerance

Recent research has highlighted the crucial role of HBV-specific $CD8^+$ T cells in the clearance of HBV.[21] In this study, we observed that $CD8^+$ T cell percentages were significantly

***Authors share co-first authorship.**

Abbreviations used in this paper: **CHB, chronic hepatitis B; HBcAg, hepatitis B core antigen; HBeAg, hepatitis B envelope antigen; HBsAg, hepatitis B surface antigen; HBV, hepatitis B virus; HPCs, hematopoietic progenitor cells; MANF, mesencephalic astrocyte-derived neurotrophic factor; ManfHep-/-, hepatocyte-specific MANF knockout mice; ManfMye-/-, myeloid-specific MANF knockout mice; MDSCs, myeloid-derived suppressor cells; M, monocytic; PCR, polymerase chain reaction; PMN, polymorphonuclear; rMANF, recombinant MANF; siMANF, siRNA targeting MANF; Tregs, regulatory T cells; WT, wild-type.**

Most current article

2352-345X
https://doi.org/10.1016/j.jcmgh.2024.05.008

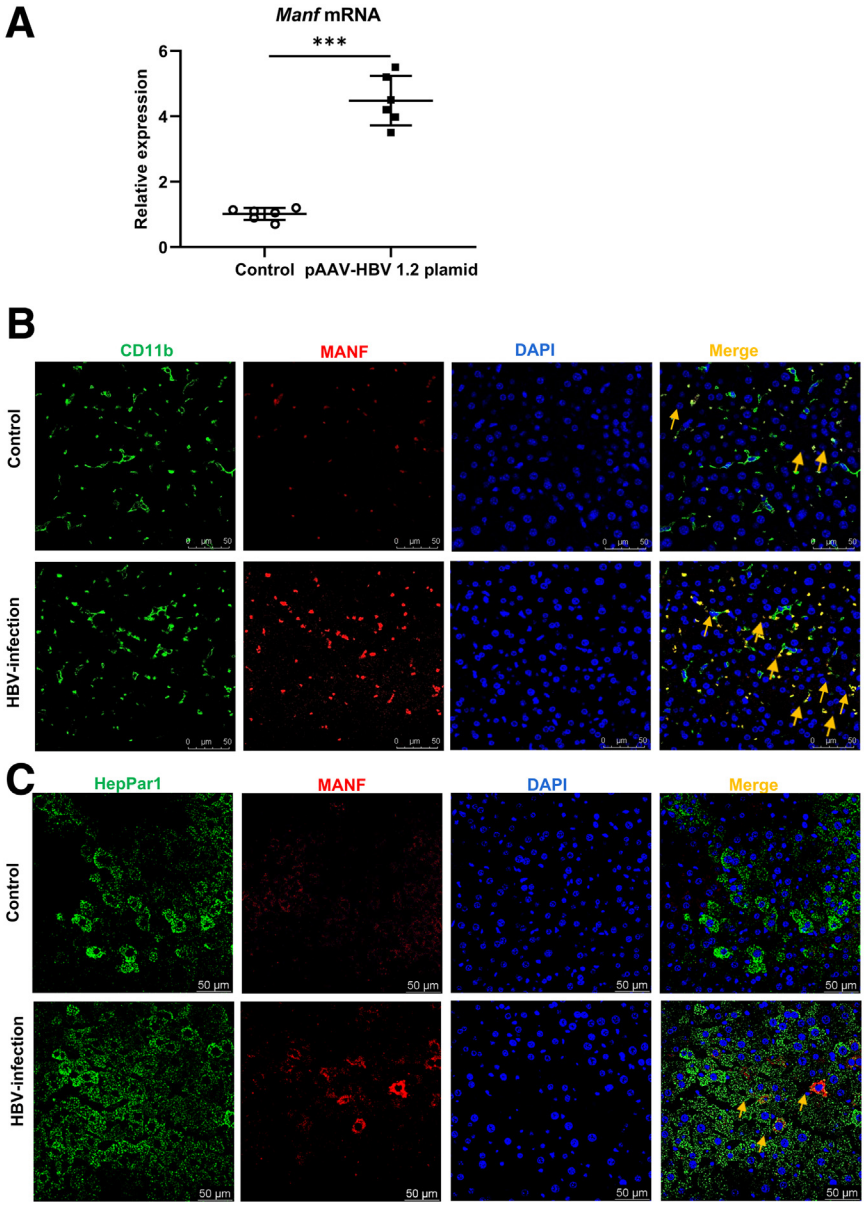

Figure 1. MANF expression was increased in the liver of HBV-positive mice. C57BL/6 mice were sacrificed 3 weeks after the pAAV/HBV1.2 plasmid injection. (*A*) Relative mRNA expression of MANF in the liver of HBV-positive C57BL/6 mice was analyzed by q-PCR. (*B*) Immunofluorescence staining for CD11b (*green*), MANF (*red*), and DAPI for nuclei (*blue*) in HBV-positive WT mice liver tissues. *Orange arrows* point to $CD11b^{+}$ myeloid cells with high expression of MANF. (*C*) Immunofluorescence staining for Hepar1 (*green*), MANF (*red*), and DAPI for nuclei (*blue*) in HBV-positive WT mice liver tissues. *Orange arrows* point to high expression MANF in hepatocytes. Each experiment was repeated at least 3 times. Data were expressed as the mean ± standard error of the mean. n = 6 mice per group. $^{*}P < .05$; $^{**}P < .01$; $^{***}P < .001$.

higher in the liver of HBV-positive $Manf^{Mye-/-}$ mice compared with HBV- positive WT mice (Figure 3*A* and *B*). Moreover, the percentage and absolute numbers of $CD11a^{hi}$ $CD8a^{lo}$ cells, which are HBV-specific $CD8^{+}$ T cells,[22,23] were also increased in the liver of HBV-positive $Manf^{Mye-/-}$ mice compared with HBV-positive WT mice (Figure 3*C*–*E*).

Furthermore, our observations revealed that hepatic $CD11a^{hi}CD8a^{lo}$ cells in HBV-positive $Manf^{Mye-/-}$ mice exhibited elevated levels of KLRG1, indicating a more pronounced effector/memory T cell phenotype, and concurrently lower levels of CD62L (Figure 3*F*). Consistent with this phenotype, the hepatic $CD11a^{hi}$ $CD8a^{lo}$ cell population displayed diminished PD-1 expression in HBV-positive $Manf^{Mye-/-}$ mice (Figure 3*F*). Additionally, we found that the proportion of hepatic $CD8^{+}$ T cells producing the antiviral cytokine IFN-γ was significantly higher in HBV-positive $Manf^{Mye-/-}$ mice compared with HBV-positive WT mice (Figure 3*G*). To further determine whether the enhanced $CD8^{+}$ T cells were sufficient to promote HBV elimination from the host, $CD8^{+}$ T cells were depleted from HBV-positive $Manf^{Mye-/-}$ mice, using an anti-CD8 mAb. Indeed, serum HBsAg levels were significantly elevated in the absence of the $CD8^{+}$ T cells (Figure 3*H*). These findings strongly suggest that the absence of myeloid MANF augments HBV-specific $CD8^{+}$ T cell responses, potentially facilitating the reversal of systemic tolerance and the eradication of HBV.

Furthermore, we observed a substantial increase in the proportion of HBV-specific $CD4^{+}$ T cells ($CD49d^{hi}$ $CD11a^{hi}$ cells) in $Manf^{Mye-/-}$ HBV-positive mice compared with WT HBV-positive mice (Figure 4*A*–*C*). Notably, we also found a

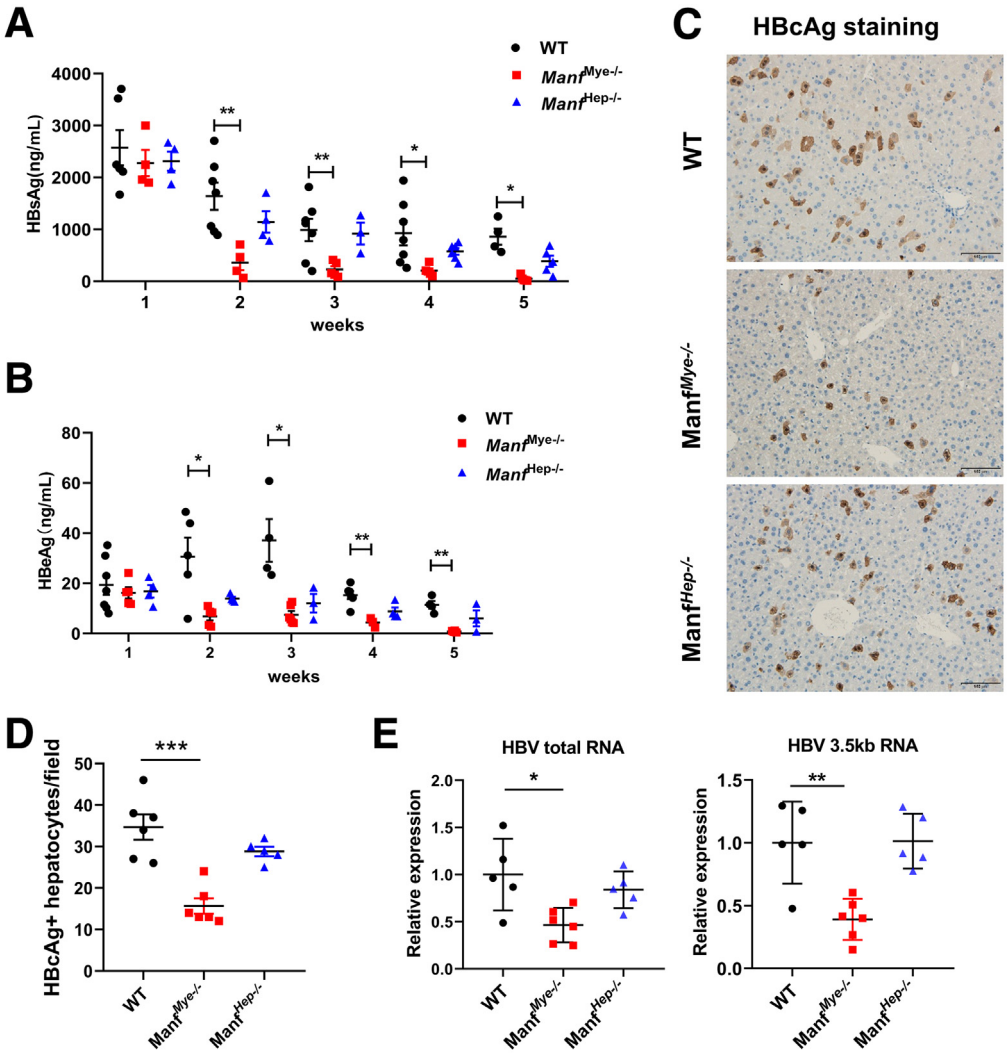

Figure 2. MANF supported the persistence of HBV in the liver. (*A and B*) WT, Manf$^{Hep-/-}$, and Manf$^{Mye-/-}$ mice were hydrodynamically injected with pAAV/HBV1.2 plasmid. Serum HBsAg and HBeAg levels were assessed by chemiluminescence immunoassay kits. (*C*) HBcAg^{+} hepatocytes in liver tissue were detected at 3 weeks post-injection by immunohistochemistry. Scale bars, 100 μm. (*D*) Quantification of HBcAg-positive cells per field. (*E*) Intrahepatic HBV total RNA and intermediate products 3.5 kb RNA in the liver were analyzed by q-PCR and normalized to β-actin 3 weeks post-injection. Experiments were repeated at least 3 times. Data were expressed as the mean ± standard error of the mean. n = 3–7 mice per group. *P < .05; **P < .01; ***P < .001.

significant reduction in PD-1 expression on CD49d^{hi} CD11a^{hi} cells in Manf$^{Mye-/-}$ HBV-positive mice (Figure 4*D*). These findings suggest that the deficiency of MANF in myeloid cells enhances not only HBV-specific CD8^{+} T cell responses but also HBV-specific CD4^{+} T cell responses, which may contribute to the overall improvement of antiviral immune responses in HBV infection.

Myeloid MANF Promotes HBV-induced Tolerance Dependent on MDSCs

We further investigated the immunosuppressive cells responsible for T-cell suppression mediated by MANF, particularly focusing on Treg cells and MDSCs known for their immunosuppressive properties in the context of HBV infection. Surprisingly, we did not observe any significant differences in the proportion of Treg cells between HBV-positive Manf$^{Mye-/-}$ mice and HBV-positive WT mice (Figure 4*E* and *F*). However, we observed a significant reduction in hepatic MDSCs in the liver of HBV-positive Manf$^{Mye-/-}$ mice compared with HBV-positive WT mice (Figure 5*A*). This reduction was observed in both M-MDSCs (CD11b^{+}Ly6G^{-}Ly6C^{high}) and PMN-MDSCs (CD11b^{+}Ly6G^{high}Ly6C^{low}) in the liver of HBV-positive Manf$^{Mye-/-}$ mice (Figure 5*B–D*).

To investigate the role of MANF in maintaining HBV tolerance through MDSCs, we performed adoptive transfer experiments using MDSCs isolated from HBV- positive WT mice to Manf$^{Mye-/-}$ mice (Figure 5*E*). Our results showed that the adoptive transfer of MDSCs was sufficient to restore high levels of HBsAg in Manf$^{Mye-/-}$ mice almost to the level observed in HBV-positive WT mice (Figure 5*F*), and reduced IFN-γ expression of CD8^{+} T cells in Manf$^{Mye-/-}$ mice (Figure 5*G*). Furthermore, we found that MANF had no impact on MDSC suppressive activity, because HBV-positive Manf$^{Mye-/-}$ mice-derived MDSCs and HBV-positive WT mice-derived MDSCs had similar expression of the genes implicated in MDSC suppressive activity and had similar repression of T cell proliferation in vitro (Figure 6*A* and *B*).

These findings suggest that the MANF-mediated maintenance of HBV tolerance is dependent on MDSCs, which act to suppress CD8^{+} T cell responses in vivo.

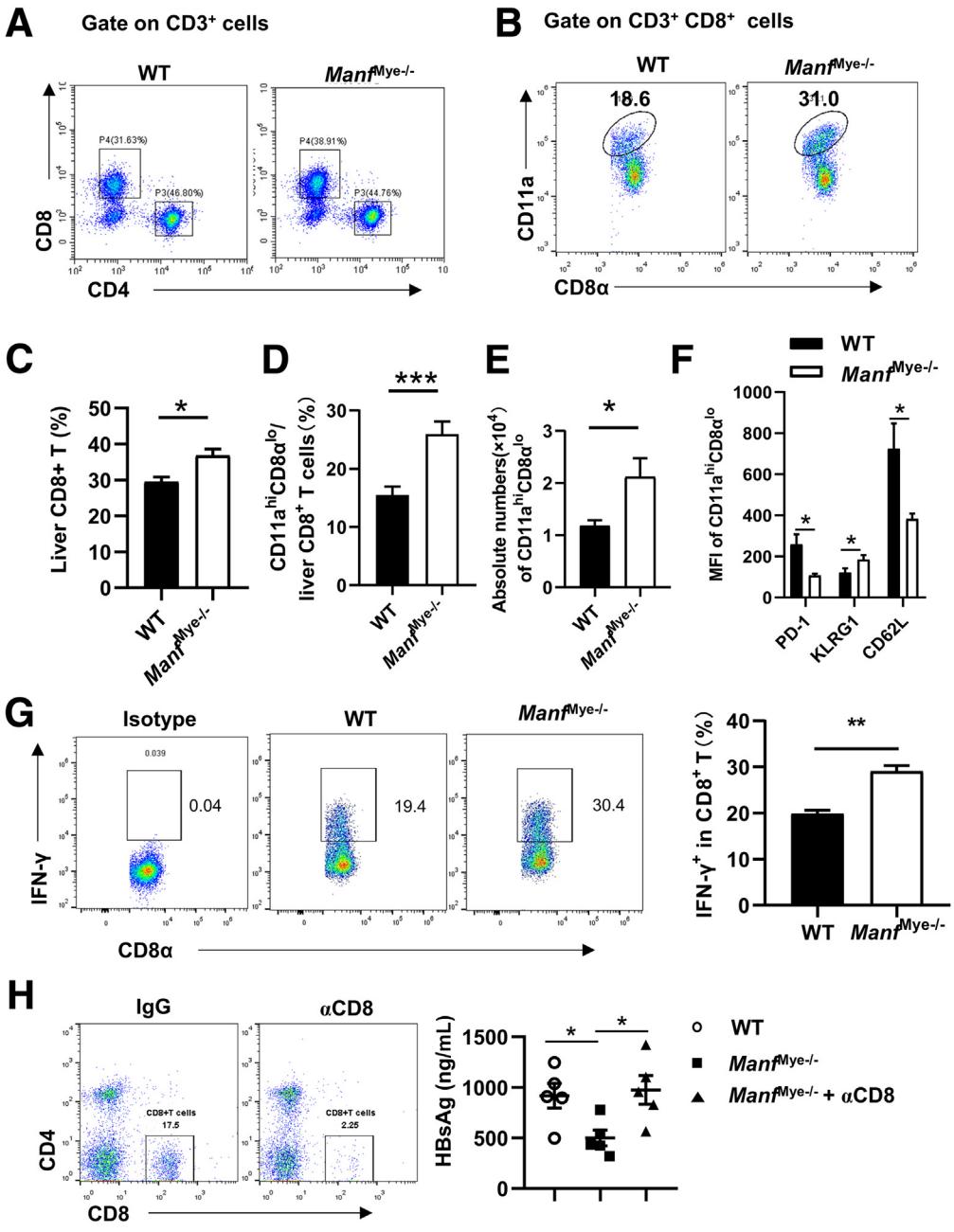

Figure 3. CD8$^+$ T cells were functionally rescued in Manf$^{Mye-/-}$ HBV-positive mice. Hepatic MNCs were isolated 3 weeks after the pAAV/HBV1.2 plasmid injection. (*A, B*) Representative flow cytometric plots of total hepatic CD8$^+$ T cells (*A*) and CD11a^{hi}CD8a^{lo} cells (*C, D*). The percentages of hepatic CD8$^+$ T cells and CD11a^{hi}CD8a^{lo} cells were calculated in the HBV-positive mice. (*E*) Numbers of CD11a^{hi}CD8a^{lo} cells in the liver were monitored. (*F*) PD-1, KLRG1, and CD62L expression on hepatic CD11a^{hi}CD8a^{lo} cells were shown. (*G*) Percentage of hepatic IFN-γ$^+$ CD8$^+$ T cells, gated on CD8$^+$ T cells. (*H*) CD8$^+$ T cells were depleted by anti-CD8 antibodies in HBV-positive Manf$^{Mye-/-}$ mice. The percentages of CD8$^+$ T cells in the liver and serum HBsAg levels were measured 3 weeks post pAAV/HBV1.2 plasmid injection. Each experiment was repeated at least 3 times. Data are expressed as the mean ± standard error of the mean. n = 4–6 mice per group. *P < .05; **P < .01; ***P < .001.

MANF Promotes MDSC Expansion via MAPK/IL-6/STAT3 Pathway

To study the mechanism underling MANF promotes MDSC expansion in the liver, we first investigated whether MANF facilitates MDSC chemotaxis. We analyzed the expression of MDSC-related chemokines including CXCL1, CXCL2, and CXCL5 in liver tissues isolated from HBV-positive mice and found that these hepatic MDSC-related chemokines were not perturbed by MANF deficiency (Figure 7*A*). This suggests that decreased MDSC numbers in the liver of HBV-positive Manf$^{Mye-/-}$ mice may not be due to increased cell chemotaxis. In addition, our results showed that hematopoietic progenitor cells (HPCs) derived from Manf$^{Mye-/-}$ mice and WT mice generated the same amount of MDSCs in the same treatment with GM-CSF and IL-6 in vitro (Figure 7*B* and *C*), suggesting that MANF deficiency did not affect the internal ability of HPCs in differentiation into MDSCs. We then examined whether MANF affects MDSC proliferation or apoptosis and found that MANF deficiency in myeloid cells did not apparently affect the apoptosis (Figure 8*A* and *B*) or proliferation (Figure 8*C* and *D*) of MDSCs derived from bone marrow or liver tissues.

We then examined the expression of local cytokines, such as CSF, SCF, IL-6, and VEGF, which can promote MDSC proliferation and expansion,[10] in liver tissues. Our results showed that IL-6 mRNA expression was decreased in the liver of HBV-positive Manf$^{Mye-/-}$ mice (Figure 9*A*).

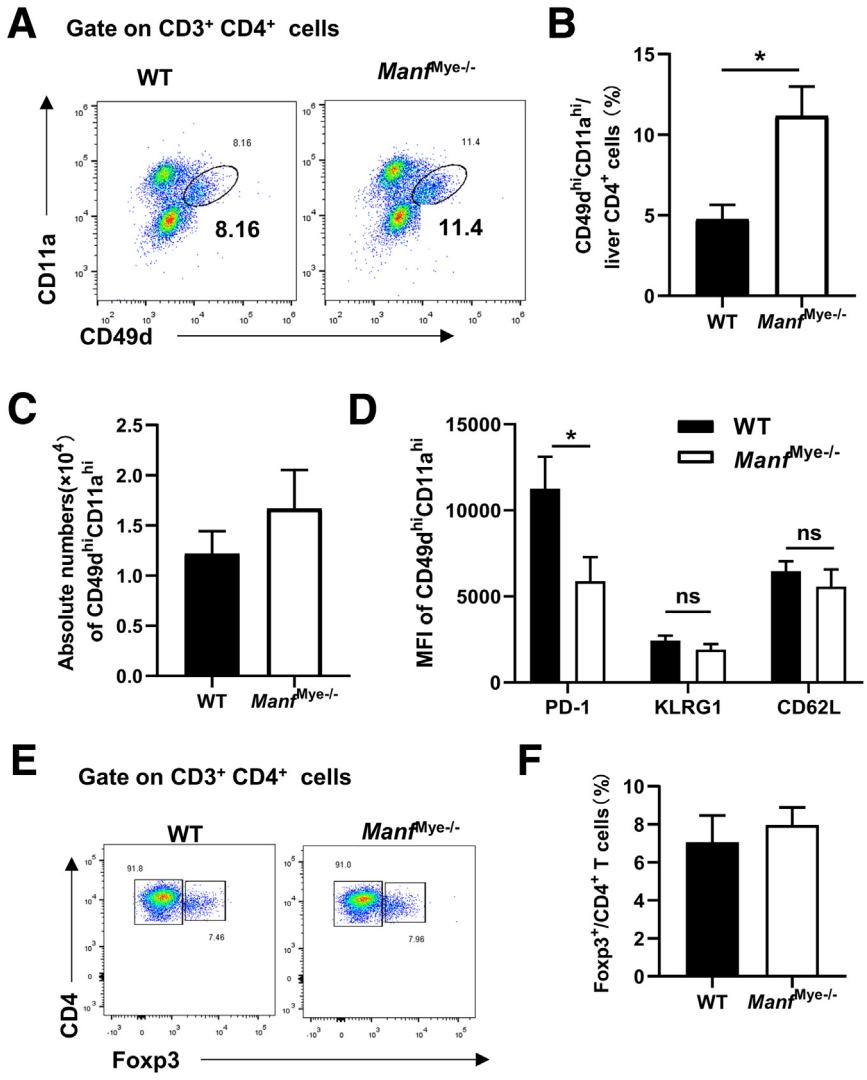

Figure 4. Analysis of HBV-specific CD4$^+$ T cells and Treg cells. Hepatic MNCs were isolated 3 weeks after the pAAV/HBV1.2 plasmid injection. (*A–C*) Percentages and numbers of CD11a-^{hi}CD49d^{hi} cells in the liver were monitored. (*D*) PD-1, KLRG1, and CD62L expression on hepatic CD11a^{hi}CD49d^{hi} cells were shown. (*E*, *F*) The percentage of hepatic CD4$^+$Foxp3$^+$ T cells was calculated. Data are expressed as the mean ± standard error of the mean. n = 4–6 mice per group. *P < .05; ns, not significant.

Additionally, recombinant MANF (rMANF) increased IL-6 mRNA levels in bone marrow cells (Figure 9*B*). Because our previous study showed that rMANF could activate the MAPK family, including JNK, p38, and ERK1/2 in peritoneal macrophages of WT mice,[16] we next examined whether MANF could enhance IL-6 expression via MAPK pathway. Our data revealed that JNK, p38, and ERK1/2 inhibitors reduced IL-6 expression (Figure 9*C*). The phosphorylation of STAT3, which is the main downstream pathway of IL-6 and can induce MDSC differentiation and expansion,[24,25] was also decreased in liver MDSCs of Manf$^{Mye-/-}$ mice as compared with WT mice (Figure 9*D*). These results suggest that MANF may affect MDSC expansion and differentiation via the MAPK/IL-6/STAT3 pathway.

siMANF-based Vaccination Therapy Successfully Limited HBV

Previous studies have shown that HBV-carrier mice mimic the immune tolerance of CHB.[26] And like CHB, HBV-carrier mice are not able to mount a humoral immune response to conventional HBV vaccination.[19,22] Thus, we used this mouse model to investigate whether a combined treatment involving siMANF could reverse the tolerant state towards peripheral HBV vaccination. This therapeutic approach, termed siMANF-based vaccination therapy (Figure 10*A*), involved the specific knockdown of MANF expression in myeloid cells using nanoparticle-encapsulated MANF siRNA, as previously described.[27] These nanoparticles were efficiently internalized by phagocytes,[28] allowing for the targeted silencing of the MANF gene in myeloid cells (Figure 10*B*). Importantly, siMANF-based vaccination therapy did not induce any noticeable liver injury (Figure 10*C*), but it did result in a remarkable decrease in serum HBsAg and HBeAg levels (Figure 10*D*). Additionally, there was a reduction in the number of HBcAg-positive hepatocytes after siMANF-based vaccination therapy (Figure 10*E*). Furthermore, hepatic MDSCs were decreased following siMANF-based vaccination therapy (Figure 10*F*). And IFN-γ expression of CD8$^+$ T cells were

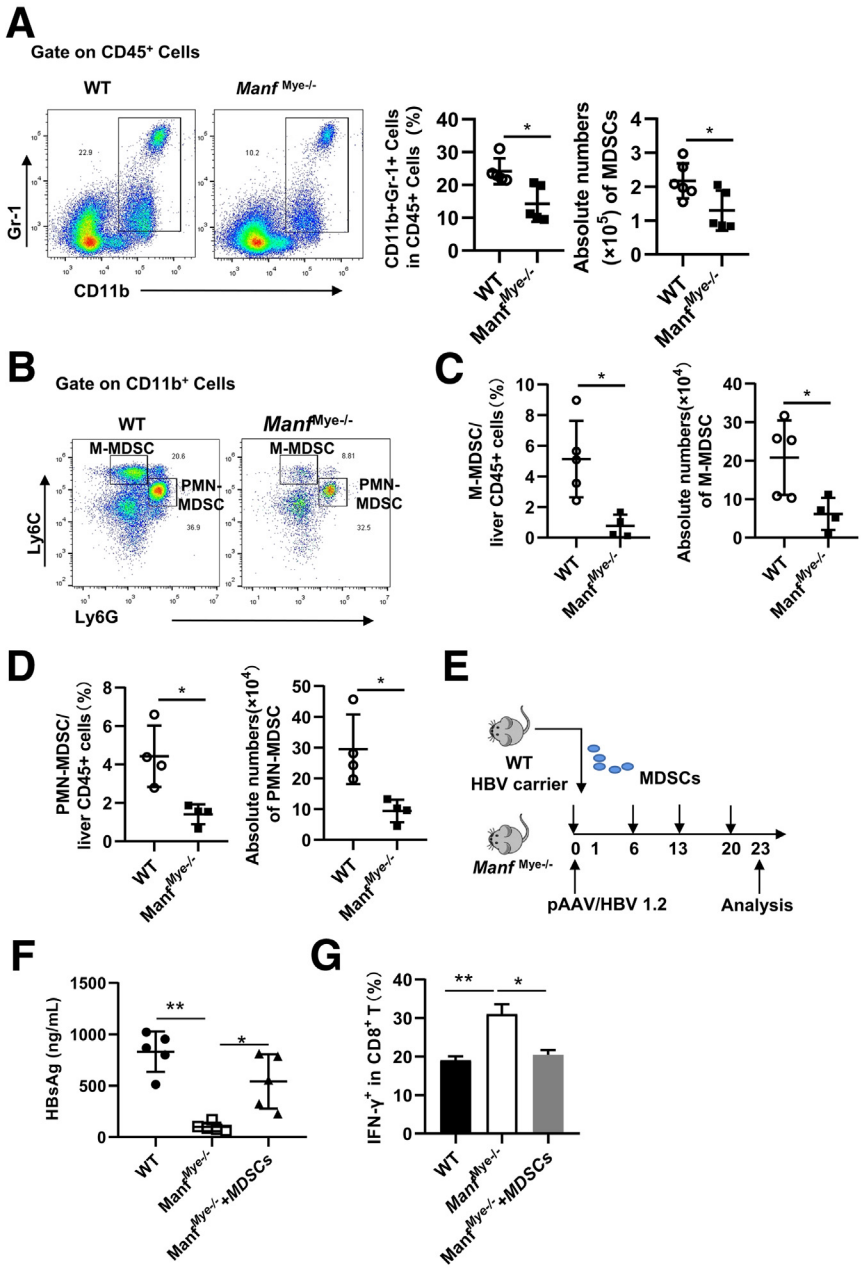

Figure 5. Myeloid MANF promotes HBV-induced tolerance via MDSCs. (*A*) The percentage and absolute number of MDSCs in liver tissues were analyzed by flow cytometry 3 weeks after pAAV/HBV1.2 plasmid injection. (*B–D*) The percentage and absolute number of PMN-MDSCs ($CD11b^+Ly6G^+Ly6C^{low}$) and M-MDSCs ($CD11b^+Ly6G^-Ly6C^{high}$) in liver tissues were analyzed by flow cytometry 3 weeks post-injection. (*E*) Schematic representation of the model of mice treatment. WT mice and $Manf^{Mye-/-}$ mice were injected with pAAV/HBV1.2 plasmid. Sorted MDSCs-derived from HBV-positive WT mice were transferred into $Manf^{Mye-/-}$ mice once a week. Mice were sacrificed on day 23 post-injection. (*F*) Serum HBsAg levels were assessed. (*G*) The percentage of hepatic IFN-γ^+ $CD8^+$ T cells was examined. Each experiment was repeated twice. Data were expressed as the mean ± standard error of the mean. n = 5–7 mice per group. $^*P < .05$; $^{**}P < .01$.

increased post siMANF-based vaccination therapy (Figure 10*G*). These results suggest that the therapy may modulate the immunosuppressive environment by targeting MDSCs, further supporting its efficacy in reversing HBV tolerance.

MANF Expression Levels of MDSCs Correlated Positively With T cell PD1 Levels in Patients With CHB

To explore the relationship between MANF expression levels of MDSCs with T cell exhaustion in patients with CHB, we selected the GSE234241 dataset. Following strict quality control, we performed UMAP-based hierarchical clustering, resulting in the identification of 15 cell subgroups (Figure 11*A*). Our further analysis showed that MANF-positive MDSCs were increased in patients with CHB compared with healthy controls, and the expression levels of MANF in MDSCs were also increased in patients with CHB (Figure 11*B*). Furthermore, MANF expression levels of MDSCs correlated positively with T cell PD1 levels in patients with CHB (Figure 11*C*).

Discussion

MANF has been implicated in various hepatic diseases, including acetaminophen-, high-fat diet-, or alcohol-induced liver diseases, and hepatocellular carcinoma.[14,29,30] Recent

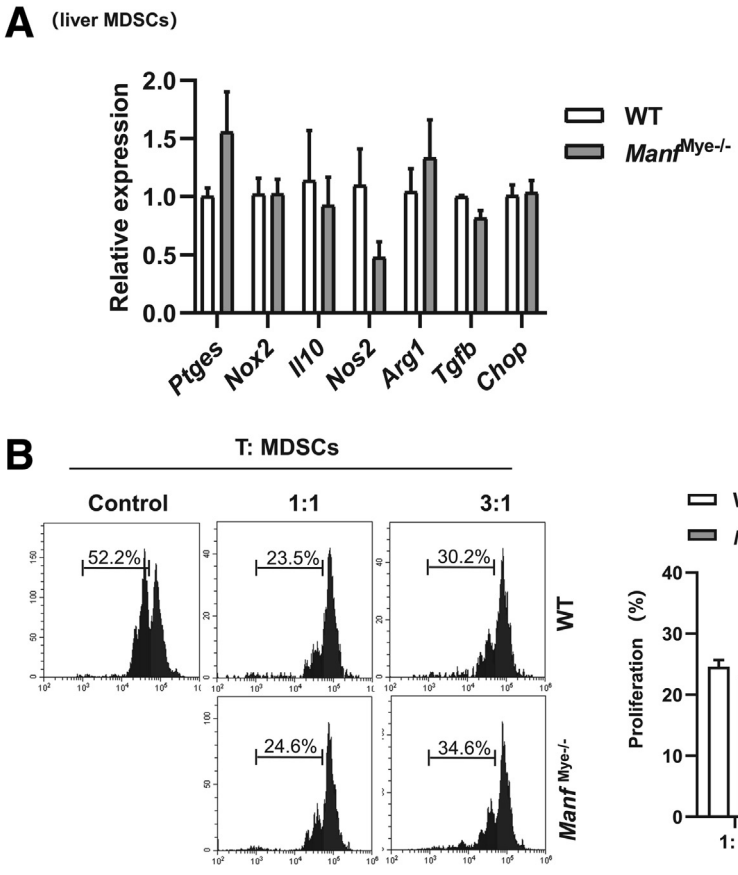

Figure 6. Myeloid MANF deficiency does not affect the suppressive activity of MDSCs in HBV-positive mice. (*A*) Hepatic MDSCs were isolated 3 weeks after pAAV/HBV1.2 plasmid injection. The expression of the indicated genes adjusted to β-actin expression was measured by qRT-PCR. (*B*) $CD8^+$ T-cell proliferation suppression assay. CFSE-labeled $CD8^+$ T cells from WT mice were stimulated with anti-CD3 and anti-CD28 antibodies and cocultured for 3 days with MDSCs isolated from WT HBV-positive and $Manf^{Mye-/-}$ HBV-positive mice at 1:1 or 3:1 ratio. Data are expressed as the mean ± standard error of the mean, n = 6 mice per group.

studies have reported increased levels of MANF in the liver tissues of patients with HBV infection,[17] yet the role of MANF in HBV infection remains unclear. In this study, we unraveled a novel function of myeloid MANF in maintaining the tolerance of HBV via promoting the expansion of MDSCs in the liver. Mechanistically, MANF enhances the MAPK/IL-6/STAT3 signaling pathway to promote MDSC expansion. Notably, MANF did not significantly impact the apoptosis, proliferation, and the suppression activity of MDSCs, as well as the differentiation of MDSCs from HPCs. Furthermore,

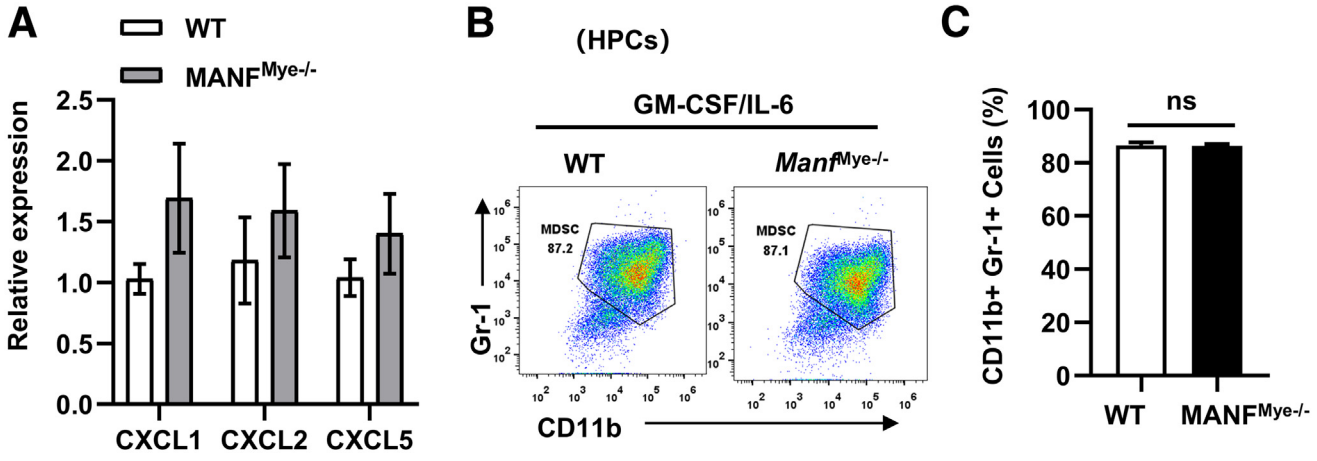

Figure 7. Myeloid MANF deficiency did not affect MDSC chemotaxis and their differentiation from HPCs in the presence of abundant GM-CSF and IL-6. (*A*) Expression of MDSC-related chemokine genes in the liver of HBV-positive mice were examined 3 weeks post pAAV/HBV1.2 plasmid injection. (*B, C*) HPCs were sorted out from $Manf^{Mye-/-}$ mice and WT mice, stimulated with GM-CSF and IL-6 for 72 hours, and the percentage of MDSCs was measured. Data are expressed as the mean ± standard error of the mean. ns, not significant.

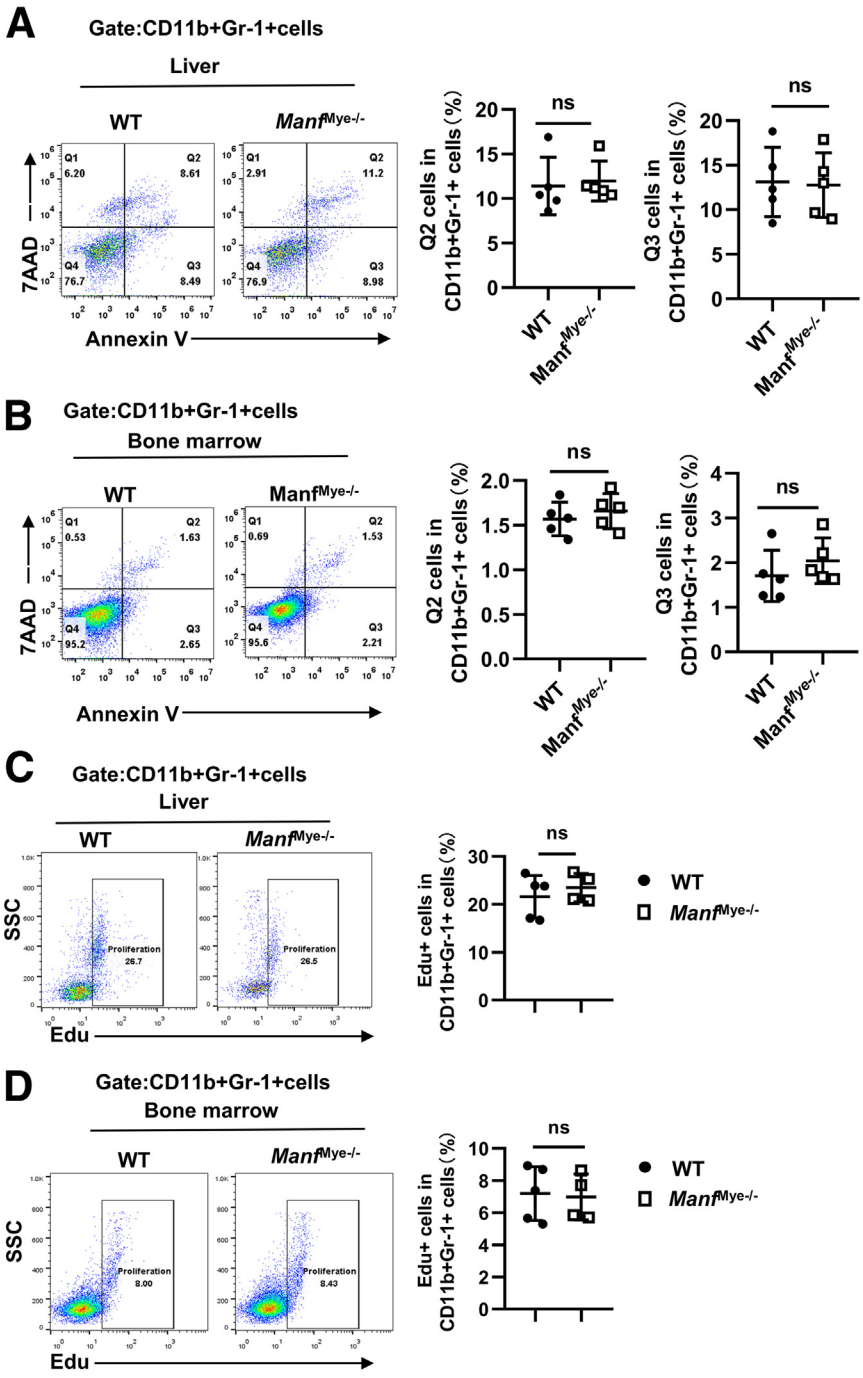

Figure 8. Myeloid MANF deficiency did not apparently affect the apoptosis and proliferation of MDSCs. (*A–D*) Manf$^{Mye-/-}$ mice and WT mice were injected with HBV1.2 plasmid via the tail vein and sacrificed after 3 weeks. (*A, B*) Flow cytometry analysis of CD45^{+}CD11b^{+}Gr1^{+} cell death using dual 7AAD and Annexin 5 staining. Q2, late apoptotic cells; Q3, early apoptotic cells. (*C, D*) Percentages of Edu^{+} cells out among CD45^{+}CD11b^{+}Gr1^{+} cells in liver tissues and bone marrow of WT and Manf$^{Mye-/-}$ mice. Data are expressed as the mean ± standard error of the mean. n = 4–6 mice per group. ns, not significant.

our findings demonstrating the successful limitation of HBV through siMANF-based vaccination therapy hold promise for the development of therapeutic vaccines against CHB carriers. These findings provide valuable insights for the design of future therapeutic interventions targeting MANF in the context of HBV infection.

We demonstrated that MANF was elevated in HBV-positive mice (Figure 1*A*). Both hepatic myeloid cells and hepatocytes exhibited increased MANF expression in response to HBV infection (Figure 1*B* and *C*). Additionally, we observed that Manf$^{Mye-/-}$ mice exhibited decreased levels of HBV components in the serum and liver (Figure 2). This effect was attributed to the rescue of CD8^{+} T cell function and the alleviation of CD8^{+} T cell exhaustion. (Figure 3). In contrast, no significant change in HBV components was observed in Manf$^{Hep-/-}$ mice compared with WT mice (Figure 2). These results suggested that the autocrine immunomodulatory function of MANF in myeloid cells was crucial for maintaining HBV-specific immune tolerance during persistent HBV infection. It is worth noting that previous

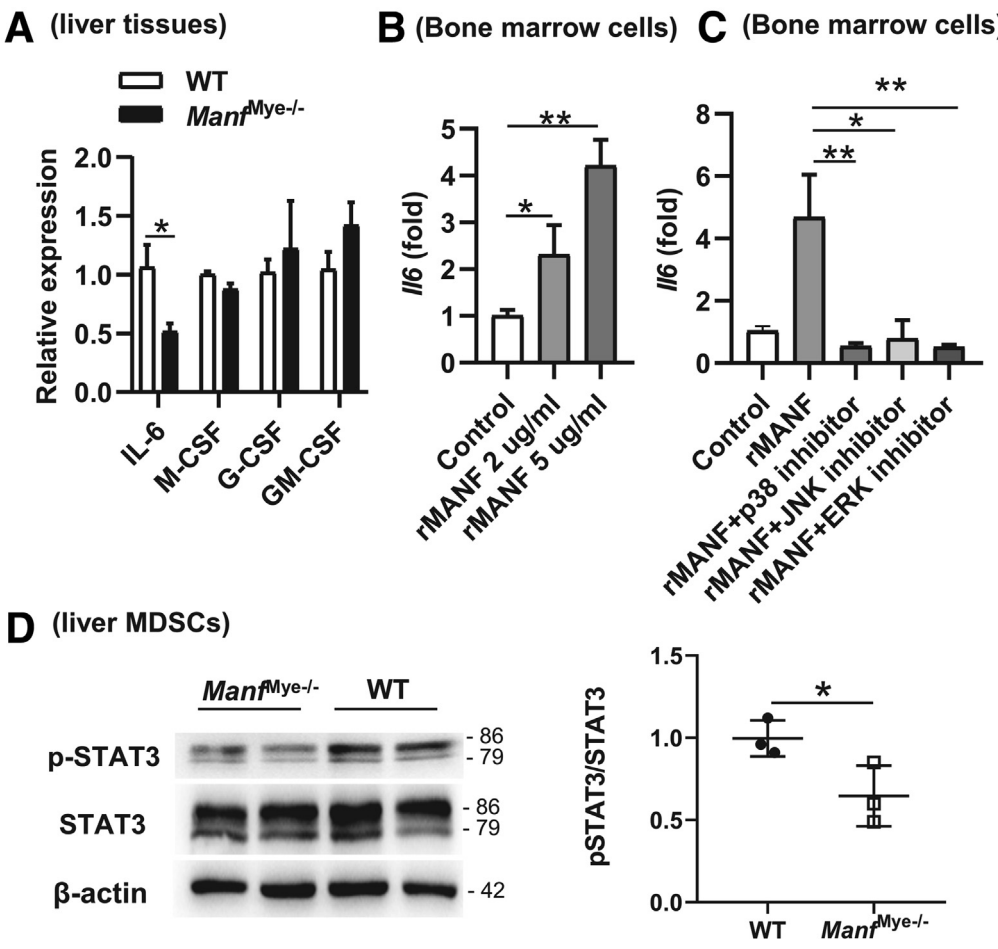

Figure 9. MANF promotes MDSC expansion in the liver via the MAPK/IL-6/STAT3 signaling pathway. (*A*) Expression of MDSC expansion-related genes in the liver of HBV-positive mice were examined 3 weeks post pAAV/HBV1.2 plasmid injection. (*B*) RT-qPCR analysis of *Il6* levels in WT bone marrow cells treated with rMANF for 6 hours. (*C*) Bone marrow cells of naive WT mice were pretreated with inhibitors for 1 hour, followed by rMANF treatment (5 μg/mL) for 6 hours. *Il6* mRNA expression was measured by RT-qPCR. (*D*) Phosphorylated and total STAT3 levels in primary liver MDSCs from WT and Manf$^{Mye-/-}$ mice 3 weeks post pAAV/HBV1.2 plasmid injection. All experiments were repeated at least 3 times. Data were expressed as the mean ± standard error of the mean. n = 4 mice per group.

studies have suggested diverse roles of MANF from different cellular sources in the aging mouse liver.[31] Immune-cell-derived MANF has been shown to protect against liver inflammation, damage, and fibrosis, whereas hepatocyte-derived MANF prevents hepatosteatosis.[31] Additionally, our previous study demonstrated that MANF derived from myeloid cells, rather than hepatocytes, contributes to the resolution of acetaminophen-induced liver injury.[16]

Our findings highlight the role of myeloid cell-derived MANF in promoting HBV-induced MDSC accumulation in the liver. In HBV-positive Manf$^{Mye-/-}$ mice, we observed a reduced number of both M-MDSCs and PMN-MDSCs (Figure 5*A*–*D*). The development of MDSCs during cancer and chronic inflammation is known to occur in 2 phases: expansion and activation.[25,32] The first phase involves the expansion of immature myeloid cells in the bone marrow and their migration to peripheral tissues. It is now recognized that a similar process occurs in peripheral tissues, where HSPCs can migrate from the bone marrow and undergo myelopoiesis locally.[33,34] This process is regulated by diverse soluble factors, including IL-6, G-CSF, and GM-CSF, and depends on the activation of transcription factors such as STAT3.[32,35] The second phase involves the activation of immature myeloid cells, leading to their conversion into functional MDSCs in peripheral tissues. This activation is driven by pro-inflammatory molecules like IFN-γ, IL-1β, TNF-α, and TLR ligands.[36,37] Our results showed that the IL-6/STAT3 signaling pathway was diminished in the liver of HBV-positive Manf$^{Mye-/-}$ mice compared with HBV-positive WT mice (Figure 9*A* and *D*). In vitro experiments further confirmed that MANF enhanced IL-6 expression in BM cells via MAPK activation (Figure 9*B* and *C*). Interestingly, we did not observe significant changes in MDSC-related chemokines in the liver tissues (Figure 7*A*), suggesting that MANF may primarily influence the first expansion phase of MDSC development, which involves myelopoiesis.

Therapeutic HBV vaccines hold promise as immunotherapies for breaking tolerance and overcoming immune exhaustion in HBV infection.[38,39] However, the development of effective therapeutic HBV vaccines has been challenging, with limited success achieved so far.[40,41] Nanoparticles have emerged as an excellent platform for vaccine development. They can mimic natural infection with pathogens and are easily taken up by antigen-presenting cells, such as macrophages and other myeloid cells. Additionally, nanovaccines can co-deliver antigens, miRNA, and adjuvants to individual antigen-presenting cells, thereby enhancing immune responses.[42] Recently, a liposome-based nanoparticle vaccine

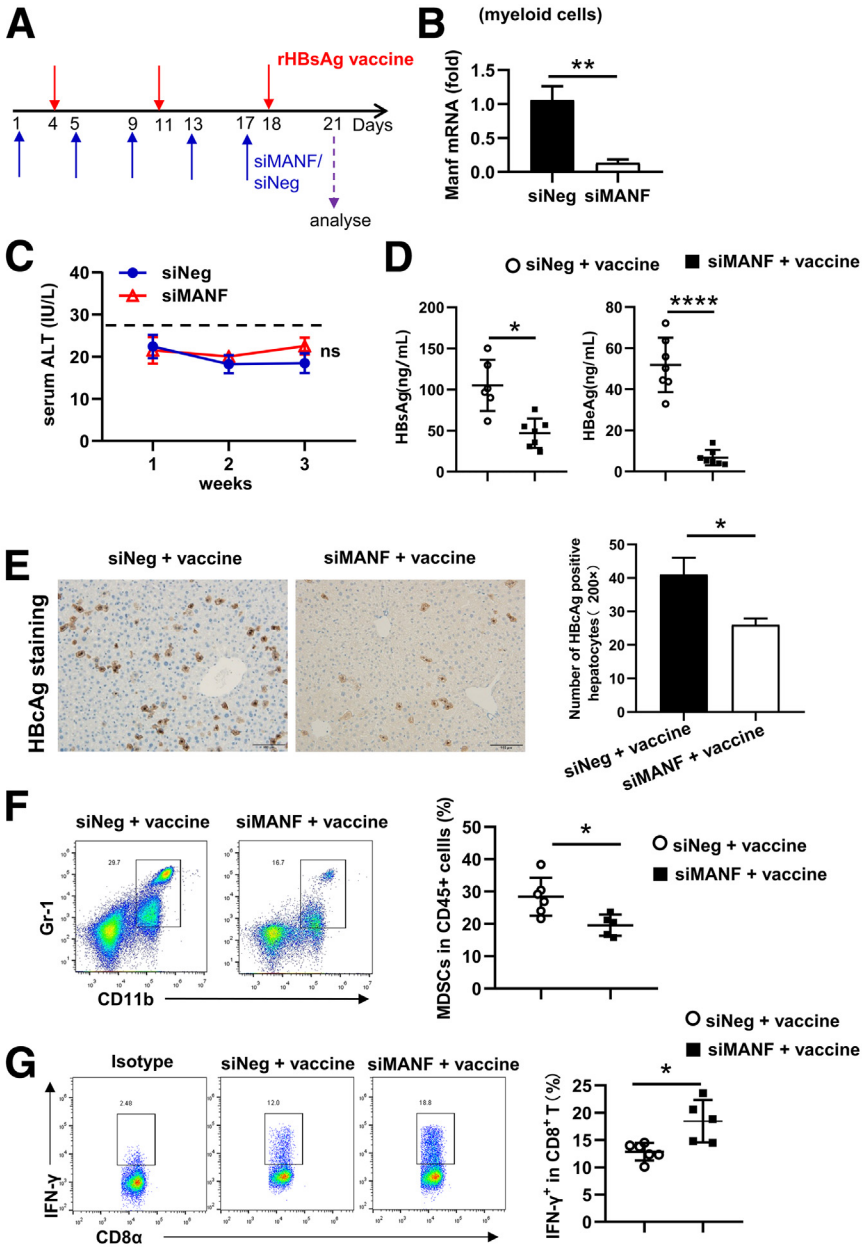

Figure 10. siMANF-based vaccination therapy successfully limited HBV. (*A*) WT mouse serum were examined 6 weeks after HBV plasmid injection, and mice with serum levels of HBsAg at least 500 ng/mL were screened out as HBV-carrier mice. These selected mice were treated with siMANF or siNeg every 4 days. rHBsAg vaccine was injected on day 4, day 11, and day 18. Mice were sacrificed on day 21 after the treatment. (*B*) MANF expression in liver myeloid cells was examined by qPCR. (*C*) Serum alanine transaminase levels were monitored during treatment. Alanine transaminase levels <28 IU/L were considered physiologically normal. (*D*) Serum HBsAg and HBeAg levels were determined in siNeg+rHBsAg vaccine–treated and siMANF+rHBsAg vaccine–treated mice. (*E*) Immunohistochemical staining of HBcAg in liver sections, and HBcAg^{+} cells per field was quantified. (*F*) The percentage of MDSCs in liver tissues was analyzed by flow cytometry. (*G*) The percentage of hepatic IFN-γ^{+} CD8^{+} T cells was examined. Each experiment was repeated twice. Data were expressed as the mean ± standard error of the mean. n = 5–7 mice per group. *P < .05; **P < .01; ****P < .0001.

(εPA-44) for CHB has completed the phase I and pilot phase II trials. The results demonstrated that εPA-44 monotherapy improved HBeAg seroconversion, reduced serum HBV load, and normalized alanine transaminase levels in patients with CHB.[43] In our study, we utilized nanoparticles to deliver siMANF to myeloid cells. The combination of siMANF with the HBsAg vaccine resulted in decreased levels of serum HBsAg and HBeAg, as well as reduced HBcAg expression in the liver (Figure 10). Notably, our siMANF-based vaccination therapy significantly reduced HBeAg levels. HBeAg seroconversion is considered a successful therapeutic outcome for HBeAg-positive patients with CHB, as it is associated with improved survival, reduced incidence of hepatocellular carcinoma, and prevention of disease progression.[43–45]

Our study provides insights into the role of myeloid MANF in maintaining liver tolerance during HBV infection by promoting the accumulation of hepatic MDSCs, which indirectly leads to CD8^{+} T cell dysfunction. Importantly, our findings demonstrate that siMANF-based vaccination therapy can reduce MDSC expansion and facilitate HBV clearance. These results suggest that targeting myeloid MANF could be a potential therapeutic strategy for the treatment of chronic HBV infection in clinical settings.

Materials and Methods

Animals

Manf$^{Hep-/-}$ and Manf$^{Mye-/-}$ mice were kindly provided by Professor Yuxian Shen of Anhui Medical University,

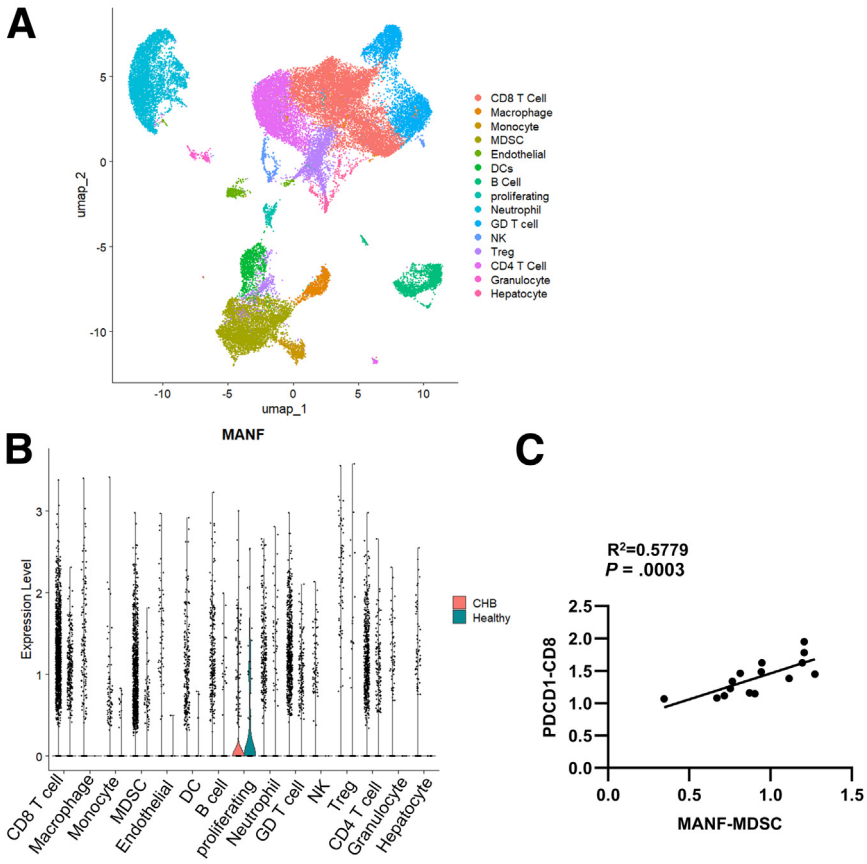

Figure 11. Analysis based on the 234241 dataset. (*A*) The UMAP of GSE234241. (B) MAFN gene expression levels in cell subsets. (*C*) The correlation between MANF expression levels in MDSC and PDCD1 expression levels in $CD8^+$ cells.

Hefei, Anhui, China. $Manf^{Hep-/-}$ and $Manf^{Mye-/-}$ mice were generated by crossing $Manf^{flox/flox}$ mice with Albumin Cre mice and Lysosome Cre mice, respectively. $Manf^{flox/flox}$ mice were used as WT mice. All mice were housed in a specific pathogen-free facility, received human care, and were used according to the animal care regulations of Ningbo University. This study was approved by the Ethics Committee of Ningbo University.

HBV-harboring Mouse Model

To establish HBV-positive mice, 5- to 6-week-old male mice were hydrodynamically injected with 6 μg pAAV/HBV1.2 via the tail vein within 5 to 8 seconds, as previously reported.[6,23] At 6 weeks after the hydrodynamic injection, the mice with serum levels of HBsAg at least 500 ng/mL were selected and defined as HBV-carrier mice.

Detection of HBV Replication

Serum levels of HBsAg and HBeAg were detected with commercial chemiluminescence immunoassay kits (Autobio) according to the manufacturer's instructions. The levels of HBV total RNA and intermediate products 3.5 kb RNA in the liver were measured by quantitative real-time polymerase chain reaction (PCR).

Quantitative Real-time PCR

Intrahepatic mRNA was extracted by TransZol Up reagent (TransGen Biotech) according to the manufacturer's instructions. First strand cDNA was synthesized using TransScript One-Step gDNA Removal and cDNA Synthesis SuperMix (TransGen Biotech). Quantitative PCR was performed using PerfectStart Green qPCR SuperMix (TransGen Biotech) on LightCycler 480II (Roche). The primer sequences are listed in Table 1.

Histology Assay

MANF expression in liver tissue was examined by immunofluorescence staining. Frozen sections were stained with rabbit anti-mouse CD11b (1/50 dilution, #46512, Cell Signaling Technology), hepatocyte-specific antibody (Hep-Par1) (1/50 dilution, #NBP2-45272, Novus), and mouse anti-mouse MANF antibody, followed by Alexa Fluor 488 Conjugate anti-rat IgG (H + L) (1/1000 dilution, #4416, Cell Signaling Technology), Alexa Fluor 488 Conjugate anti-mouse IgG (H + L) (1/1000 dilution, #4408, Cell Signaling Technology), Rhodamine conjugated goat anti-mouse IgG (H + L) (1/100 dilution, ZSGB-BIO, ZF0313), and 4′, 6′-diamino-2-phenylindole (DAPI). Images were acquired on a Leica TCS SP8 confocal microscope. $HBcAg^+$ hepatocytes in liver tissue were examined by immunohistochemistry

Table 1. RT-qPCR primer sequences

Gene	Primer	Sequence (5′-3′)
Manf	Forward	CACCAGCCACTATTGAAGAAGA
	Reverse	AGCATCATCTGTGGCTCCAA
HBV-total-RNA	Forward	TCACCAGCACCATGCAAC
	Reverse	AAGCCACCCAAGGCACAG
HBV-3.5kb RNA	Forward	GAGTGTGGATTCGCACTCC
	Reverse	GAGGCGAGGGAGTTCTTCT
Il6	Forward	ACACATGTTCTCTGGGAAATCGT
	Reverse	AAGTGCATCATCGTTGTTCATACA
Cxcl1	Forward	GCTTGAAGGTGTTGCCCTCAG
	Reverse	AAGCCTCGCGACCATTCTTG
Cxcl2	Forward	CGCTGTCAATGCCTGAAG
	Reverse	GGCGTCACACTCAAGCTCT
Cxcl5	Forward	GGTCCACAGTGCCCTACG
	Reverse	GCGAGTGCATTCCGCTTA
M-csf	Forward	ATGAGCAGGAGTATTGCCAAGG
	Reverse	TCCATTCCCAATCATGTGGCTA
G-csf	Forward	TGCTTAAGTCCCTGGAGCAA
	Reverse	AGCTTGTAGGTGGCACACAA
Gm-csf	Forward	GGCCTTGGAAGCATGTAGAGG
	Reverse	GGAGAACTCGTTAGAGACGACTT
Arg1	Forward	AACACGGCAGTGGCTTTAACC
	Reverse	GGTTTTCATGTGGCGCATTC
inos	Forward	GTTCTCAGCCCAACAATACAAGA
	Reverse	GTGGACGGGTCGATGTCAC
Actin	Forward	CCTTCTTGGGTATGGAATCCTGT
	Reverse	GGCATAGAGGTCTTTACGGATGT
Nos2	Forward	TGTGGCTGTGCTCCATAGTT
	Reverse	CTGGAGGGACCAGCCAAATC
Arg1	Forward	AACACGGCAGTGGCTTTAACC
	Reverse	GGTTTTCATGTGGCGCATTC
Ptges	Forward	GCACACTGCTGGTCATCAAG
	Reverse	ACGTTTCAGCGCATCCTC
Il10	Forward	GCAGGACTTTAAGGGTTACTTGG
	Reverse	CACCTTGGTCTTGGAGCTTATTAA
Nox2	Forward	CAGTGCTGACCCAAGGAGTT
	Reverse	GGGAACTGGGCTGTGAATGA
Tgfb	Forward	AGCTGCGCTTGCAGAGATTA
	Reverse	ATTCCGTCTCCTTGGTTCAGC
Chop	Forward	CTGCCTTTCACCTTGGAGAC
	Reverse	CGTTTCCTGGGGATGAGATA

staining with rabbit anti-HBcAg (Quartett GmbH). Images were taken with an Olympus microscope.

Flow Cytometry

The mAb used in this study included PE-CY7-anti-CD3, BV510-anti-CD45, PerCP/CY5.5-anti-CD4, FITC-anti-CD8a, APC-anti-CD11a, BV421-anti-CD49d, PE-anti-IFN-γ, APC/CY7-anti-TNF-α, FITC-anti-Ly6C, PE-anti-CD68, PerCP/CY5.5-anti-F4/80, PE/CY7-anti-CD45, FITC-anti-CD11b, V450-anti-Gr-1, PD1, KLRG1, CD62L, MHC-II. PE-CY7-Ki67, Percpcy5.5-7AAD, and PE-Annexin5 (BD Pharmingen). Cells were examined by flow cytometry with a Beckman flow cytometer and analyzed with FlowJo 11.0.

Adoptive Transfer of MDSCs

For isolated hepatic MDSCs, liver leukocytes were separated by 40% Percoll (GE Healthcare) solution and collected; red blood cells were then lysed. Collected

leukocytes were further applied to Myeloid-Derived Suppressor Cell Isolation Kit, mouse (Miltenyi Biotec) to isolate MDSCs. Sorted MDSCs (3×10^6 cells per mouse) were transferred into HBV-positive $Manf^{Mye-/-}$ mice.

Western Blotting

Hepatic $CD11b^+$ cells were isolated using PE-anti-CD11b Abs (BD Pharmingen) and anti-PE microbeads (Miltenyi Biotec). Harvested cells were homogenized in RIPA buffer supplemented with the protease inhibitor cocktail (Roche). Primary Abs rabbit anti-mouse β-actin (Proteintech), rabbit anti-mouse p-stat3(Cat# 9145T, Cell Signaling), and rabbit anti-mouse Stat3 (Cat#4904T, Cell Signaling) were used to incubate NC membranes (Beyotime) at 4 °C overnight. Then membranes were incubated with peroxidase-conjugated goat anti-rabbit IgG (ZB-2301) (ZSGB-BIO). Protein bands were visualized with a chemiluminescence detection system (Tanon-5300M).

T-cell Depletion and Suppression Assays

For $CD8^+$ T depletion, anti-CD8 antibodies (BioXcel, clone:53-6.7) were administered into HBV-positive mice by intraperitoneal injection (0.2 mg/mouse) on days −2 and 8.

For T cell suppression assay, spleen $CD8^+$ T cells were purified using PE-anti-CD8 and anti-PE beads (Miltenyi Biotec). Then $CD8^+$ T cells labelled with CFSE (0.5 μM) in pre-warmed phosphate buffered saline for 20 minutes at 37 °C. The CFSE-labeled T cells were then stimulated with anti-mouse CD3 (1 μg/ml, clone 145-2C11, eBioscience) and anti-mouse CD28 (3 μg/ml, clone 37.51, eBioscience) antibodies in 96-well plates (2.5×10^4 cells per well). Liver MDSCs were isolated using Myeloid-Derived Suppressor Cell Isolation Kit (Miltenyi Biotec). Purified MDSCs were added in plates at indicated ratios. After 72 hours, cells were harvested, and CFSE signal in the gated $CD8^+$ T cells was measured by flow cytometry.

Generation of MDSCs From Sorted HPCs and Treatments

HPCs were isolated from the bone marrow of C57BL/6 mice using EasySep Mouse Hematopoietic Progenitor Cell Isolation Kit (STEMCELL Technologies). To differentiate HPCs into MDSCs, 2×10^5 isolated HPCs were placed in 24-well plates and cultured in SFEM (STEMCELL Technologies) medium containing 10 ng/mL GM-CSF (Sino Biological) and 10 ng/ml IL-6 (Sino Biological) for 72 hours, and the newly generated $CD11b^+Gr\text{-}1^+$ cells were analyzed.

Treatment of Mice With Nanoparticle-encapsulated siRNA and HBsAg Vaccine

To silence the expression of MANF on myeloid cells in HBV-carrier mouse, siMANF (sense 5′- GGCAAAGAGAAUCGG UUGUTT-3′-and antisense 5′- ACAACCGAUUCUCUUUGCCTT-3′) was designed and synthetized by GenePharma (Shanghai, China). siMANF or siNeg was encapsulated into Cationic, lipid-assisted poly (ethylene glycol)-b-poly(d,l-lactide) (PEG-PLA) nanoparticles by Guangzhou Kelan Biotechnology Co., Ltd. Recombinant HBV vaccine (Hansenula polymorpha) and HBsAg (H. polymorpha) were purchased from Dalian Hissen Bio-pharm. Co. Ltd.

Nanoparticle-encapsulated siMANF or siNeg (40 μg per mouse) was administered to HBV-carrier mice every 4 days by intravenous injection. Recombinant HBsAg vaccine (2 μg per mouse) was subcutaneously injected to mice weekly for 3 weeks.

Statistical Analysis

Statistical analysis comparing 2 groups was performed using the nonparametric or Student *t*-test, whereas analysis of variance was used when more than 2 groups were compared. Statistical analyses were performed using GraphPad Prism 8, and the data are presented as the means ± standard errors of the mean. P values $< .05$ were considered significant.

References

1. Fanning GC, Zoulim F, Hou J, Bertoletti A. Therapeutic strategies for hepatitis B virus infection: towards a cure. Nat Rev Drug Discov 2019;18:827–844.
2. Trepo C, Chan HL, Lok A. Hepatitis B virus infection. Lancet 2014;384:2053–2063.
3. Cheng Y, Zhu YO, Becht E, et al. Multifactorial heterogeneity of virus-specific T cells and association with the progression of human chronic hepatitis B infection. Sci Immunol 2019;4:eaau6905.
4. Das A, Hoare M, Davies N, et al. Functional skewing of the global CD8 T cell population in chronic hepatitis B virus infection. J Exp Med 2008;205:2111–2124.
5. Baudi I, Kawashima K, Isogawa M. HBV-Specific CD8+ T-cell tolerance in the liver. Front Immunol 2021;12:721975.
6. Kong X, Sun R, Chen Y, et al. GammadeltaT cells drive myeloid-derived suppressor cell-mediated CD8+ T cell exhaustion in hepatitis B virus-induced immunotolerance. J Immunol 2014;193:1645–1653.
7. Bronte V, Brandau S, Chen SH, et al. Recommendations for myeloid-derived suppressor cell nomenclature and characterization standards. Nat Commun 2016;7:12150.
8. Huang A, Zhang B, Yan W, et al. Myeloid-derived suppressor cells regulate immune response in patients with chronic hepatitis B virus infection through PD-1-induced IL-10. J Immunol 2014;193:5461–5469.
9. Huang S, Wang Z, Zhou J, et al. EZH2 inhibitor GSK126 suppresses antitumor immunity by driving production of myeloid-derived suppressor cells. Cancer Res 2019;79:2009–2020.
10. Li H, Tsokos MG, Bhargava R, et al. IL-23 reshapes kidney resident cell metabolism and promotes local kidney inflammation. J Clin Invest 2021;131:e142428.
11. Yang F, Yu X, Zhou C, et al. Hepatitis B e antigen induces the expansion of monocytic myeloid-derived suppressor cells to dampen T-cell function in chronic hepatitis B virus infection. PLoS Pathog 2019;15:e1007690.
12. Fang Z, Zhang Y, Zhu Z, et al. Monocytic MDSCs homing to thymus contribute to age-related CD8+ T cell tolerance of HBV. J Exp Med 2022;219:e20211838.

13. Pal S, Dey D, Chakraborty BC, et al. Diverse facets of MDSC in different phases of chronic HBV infection: impact on HBV-specific T-cell response and homing. Hepatology 2022;76:759–774.
14. Deng H, Zhang P, Gao X, et al. Emerging trophic activities of mesencephalic astrocyte-derived neurotrophic factor in tissue repair and regeneration. Int Immunopharmacol 2022;114:109598.
15. Neves J, Zhu J, Sousa-Victor P, et al. Immune modulation by MANF promotes tissue repair and regenerative success in the retina. Science 2016;353:aaf3646.
16. Hou X, Liu Q, Gao Y, et al. Mesencephalic astrocyte-derived neurotrophic factor reprograms macrophages to ameliorate acetaminophen-induced acute liver injury via p38 MAPK pathway. Cell Death Dis 2022;13:100.
17. Wang D, Hou C, Cao Y, et al. XBP1 activation enhances MANF expression via binding to endoplasmic reticulum stress response elements within MANF promoter region in hepatitis B. Int J Biochem Cell Biol 2018;99:140–146.
18. Wang CH, Jiang TC, Qiang WM, et al. Activator protein-1 is a novel regulator of mesencephalic astrocyte-derived neurotrophic factor transcription. Mol Med Rep 2018; 18:5765–5774.
19. Xu L, Yin W, Sun R, et al. Kupffer cell-derived IL-10 plays a key role in maintaining humoral immune tolerance in hepatitis B virus-persistent mice. Hepatology 2014; 59:443–452.
20. Li M, Sun R, Xu L, et al. Kupffer cells support hepatitis B virus-mediated CD8+ T cell exhaustion via hepatitis B core antigen-TLR2 interactions in mice. J Immunol 2015; 195:3100–3109.
21. Zhang C, Li J, Cheng Y, et al. Single-cell RNA sequencing reveals intrahepatic and peripheral immune characteristics related to disease phases in HBV-infected patients. Gut 2023;72:153–167.
22. Zeng Z, Kong X, Li F, et al. IL-12-based vaccination therapy reverses liver-induced systemic tolerance in a mouse model of hepatitis B virus carrier. J Immunol 2013;191:4184–4193.
23. Zhao HJ, Han QJ, Wang G, et al. Poly I:C-based rHBVvac therapeutic vaccine eliminates HBV via generation of HBV-specific CD8(+) effector memory T cells. Gut 2019;68:2032–2043.
24. Chalmin F, Ladoire S, Mignot G, et al. Membrane-associated Hsp72 from tumor-derived exosomes mediates STAT3-dependent immunosuppressive function of mouse and human myeloid-derived suppressor cells. J Clin Invest 2010;120:457–471.
25. Condamine T, Gabrilovich DI. Molecular mechanisms regulating myeloid-derived suppressor cell differentiation and function. Trends Immunol 2011;32:19–25.
26. Huang LR, Wu HL, Chen PJ, Chen DS. An immunocompetent mouse model for the tolerance of human chronic hepatitis B virus infection. Proc Natl Acad Sci U S A 2006;103:17862–17867.
27. Hou X, Hao X, Zheng M, et al. CD205-TLR9-IL-12 axis contributes to CpG-induced oversensitive liver injury in HBsAg transgenic mice by promoting the interaction of NKT cells with Kupffer cells. Cell Mol Immunol 2017; 14:675–684.
28. Cui K, Yan G, Xu C, et al. Invariant NKT cells promote alcohol-induced steatohepatitis through interleukin-1beta in mice. J Hepatol 2015;62:1311–1318.
29. Wu T, Liu QH, Li YP, et al. Feeding-induced hepatokine, Manf, ameliorates diet-induced obesity by promoting adipose browning via p38 MAPK pathway. J Exp Med 2021;218:e20201203.
30. Liu J, Wu Z, Han D, et al. Mesencephalic astrocyte-derived neurotrophic factor inhibits liver cancer through small ubiquitin-related modifier (SUMO)ylation-related suppression of NF-kappaB/Snail signaling pathway and epithelial-mesenchymal transition. Hepatology 2020; 71:1262–1278.
31. Sousa-Victor P, Neves J, Cedron-Craft W, et al. MANF regulates metabolic and immune homeostasis in ageing and protects against liver damage. Nat Metab 2019; 1:276–290.
32. Gabrilovich DI, Ostrand-Rosenberg S, Bronte V. Coordinated regulation of myeloid cells by tumours. Nat Rev Immunol 2012;12:253–268.
33. Strauss L, Sangaletti S, Consonni FM, et al. RORC1 regulates tumor-promoting "emergency" granulo-monocytopoiesis. Cancer Cell 2015;28:253–269.
34. Cortez-Retamozo V, Etzrodt M, Newton A, et al. Origins of tumor-associated macrophages and neutrophils. Proc Natl Acad Sci U S A 2012;109:2491–2496.
35. Li ZW, Sun B, Gong T, et al. GNAI1 and GNAI3 reduce colitis-associated tumorigenesis in mice by blocking IL6 signaling and down-regulating expression of GNAI2. Gastroenterology 2019;156:2297–2312.
36. Gabrilovich DI. Myeloid-derived suppressor cells. Cancer Immunol Res 2017;5:3–8.
37. Al Sayed MF, Amrein MA, Buhrer ED, et al. T-cell-secreted TNFalpha induces emergency myelopoiesis and myeloid-derived suppressor cell differentiation in cancer. Cancer Res 2019;79:346–359.
38. Cargill T, Barnes E. Therapeutic vaccination for treatment of chronic hepatitis B. Clin Exp Immunol 2021; 205:106–118.
39. Kosinska AD, Bauer T, Protzer U. Therapeutic vaccination for chronic hepatitis B. Curr Opin Virol 2017;23:75–81.
40. Lok AS, Pan CQ, Han SH, et al. Randomized phase II study of GS-4774 as a therapeutic vaccine in virally suppressed patients with chronic hepatitis B. J Hepatol 2016;65:509–516.
41. Xu DZ, Wang XY, Shen XL, et al, YIC Efficacy Trial Study Team. Results of a phase III clinical trial with an HBsAg-HBIG immunogenic complex therapeutic vaccine for chronic hepatitis B patients: experiences and findings. J Hepatol 2013;59:450–456.
42. Qiao D, Chen Y, Liu L. Engineered therapeutic nanovaccine against chronic hepatitis B virus infection. Biomaterials 2021;269:120674.
43. Wei L, Zhao T, Zhang J, et al. Efficacy and safety of a nanoparticle therapeutic vaccine in patients with chronic hepatitis B: a randomized clinical trial. Hepatology 2022; 75:182–195.
44. Hui CK, Leung N, Shek TW, et al. Hong Kong Liver Fibrosis Study Group. Sustained disease remission after spontaneous HBeAg seroconversion is associated with

reduction in fibrosis progression in chronic hepatitis B Chinese patients. Hepatology 2007;46:690–698.

45. Moucari R, Korevaar A, Lada O, et al. High rates of HBsAg seroconversion in HBeAg-positive chronic hepatitis B patients responding to interferon: a long-term follow-up study. J Hepatol 2009;50:1084–1092.

Received October 10, 2023. Accepted May 10, 2024.

Correspondence
Address correspondence to: Xin Hou, Ph.D. Health Science Center, Ningbo University, Ningbo, China, 818 Fenghua Road, Ningbo 315211, China. e-mail: houxin@nbu.edu.cn.

Acknowledgments
The authors thank the Core Facilities, Health Science Center, Ningbo University, and Laboratory Animal Center of Ningbo University for the technical support.

CRediT Authorship Contributions
Xin Hou (Funding acquisition: Lead; Supervision: Lead; Writing – review & editing: Lead)
Huiyuan Xie (Data curation: Equal; Formal analysis: Equal; Project administration: Equal; Writing – original draft: Equal)
Haiyan Deng (Data curation: Equal; Formal analysis: Equal; Methodology: Equal; Writing – original draft: Equal)
Xianxian Gao (Investigation: Supporting; Software: Supporting)
Weiyi Chen (Investigation: Supporting; Methodology: Supporting)
Yixuan Wang (Investigation: Supporting; Methodology: Supporting)
Naibin Yang (Resources: Supporting)
Liang Yong (Formal analysis: Supporting; Investigation: Supporting; Methodology: Supporting)

Conflicts of interest
The authors disclose no conflicts.

Funding
This work was supported by the grants from National Natural Science Foundation of China (82170603, 81870410) and Zhejiang Provincial Natural Science Foundation (LY22H030006).